Vibrational Assignment of All 46 Fundamentals of C_{60} and C_{60}^{6-}: Scaled Quantum Mechanical Results Performed in Redundant Internal Coordinates and Compared to Experiments

Cheol Ho Choi and Miklos Kertesz*

Department of Chemistry, Georgetown University, Washington, D.C. 20057-1227

Laszlo Mihaly

Department of Physics and Astronomy, SUNY Stony Brook, New York 11794-3800

Received: April 29, 1999; In Final Form: October 18, 1999

Traditional vibrational assignment in terms of bond stretching, angle bending, and torsion is not possible in fullerenes due to the very large number of coupled internal coordinates. Large scale density functional calculations of the vibrational properties of C_{60} and C_{60}^{6-} have been carried out with Becke3LYP and BeckeLYP exchange-correlation functionals in the pursuit of obtaining a reliable set of 174 normal modes (46 fundamental frequencies) and understanding the effect of charge transfer (doping) on the vibrational modes. The calculations involve scaling of the force field in redundant internal coordinates as proposed by Pulay et al. The scaled quantum mechanical (SQM) calculations yield excellent agreement with experiment for the 14 allowed frequencies. This provides the basis for an accurate assignment of all nonallowed fundamentals and the reassignment of the observed overtone and combination bands of the high-resolution Raman (Wang et al., 1993) and IR (Martin et al. 1994) spectra. The calculated intensity ratios for the four IR active bands agree with experiment. The large IR intensity enhancements observed for C_{60}^{6-} relative to C_{60} are explained by the enhancement of certain components of the atomic polar tensor that is partially due to bond equalization in the charged fullerene. This enhancement appears to be largely a molecular rather then a solid state effect.

Introduction

Ever since the discovery of icosahedral C_{60} in 1985,[1] fullerenes have become one the most studied materials.[2] Characterization of fullerenes requires complete vibrational assignment compatible with the experimental data.[3−7,9−14] C_{60} has 4 IR-active vibrational bands of F_{1u} symmetry and 10 Raman-active bands: 2 with A_g and 8 with H_g symmetry. All of these 14 bands have been experimentally observed and assigned with certainty,[2] except for one.[3,4]

A number of attempts to assign the other 32 fundamental frequencies can be found in the literature,[5−16] some unequivocal, others in conflict with each other and/or with earlier theoretical calculations.[17−22] A quick overview of these will serve as an introduction to and motivation for the present work. The 32 IR and Raman forbidden bands correspond to the $1A_u$, $3F_{1g}$, $4F_{2g}$, $5F_{2u}$, $6G_g$, $6G_u$, and $7H_u$ symmetry species. These "silent" modes show up in lower resolution in inelastic neutron scattering and electron scattering experiments, leading to some tentative assignments.[5] Wang et al.[6] and Martin et al.[7] have reported a complete set of the 46 fundamentals and their group-theory-allowed second-order combination bands on the basis of high-resolution measurements of C_{60} single crystals. In a related study, Martin et al. also showed[8] that ^{13}C isotope substitution cannot account for the large number of small intensity bands making it possible to assign them as combination bands.

Further important experimental information has been obtained by Coulombeau et al.[2g] using inelastic neutron scattering. Nissen et al.[9] and Heid et al.[10] reported a wealth of information on the vibronic spectrum of C_{60} using O_2 photoluminescence. Sassara et al.[11] have done fluorescence and phosphorescence measurements which combined with early valence force field calculations of Negri et al.[24] yielded several assignments that were confirmed later, including the assignment presented in this work.

In spite of extensive experimental efforts, definite vibrational assignment for some spectroscopically inactive modes remains incomplete due to the numerous sources of uncertainties such as isotope effects, anharmonicity, combination bands, overtones, symmetry breaking, solvent effect and even impurities.

A different way to obtain further information is based on the comparison of the spectra of pristine C_{60} with those under pressure[8] in the dimerized[12] or polymerized[13] phases, or those of compounds of C_{60} (Long et al.[13]) An interesting attempt to assign the silent modes was made by Cardini et al.[14] by using $C_{60}O$ and $C_{61}H_2$ molecules in order to break the I_h symmetry so as to activate silent modes. These modified spectra indicate the presence of fundamentals and aid the assignment in a particular frequency range but the actual values of the frequencies are shifted relative to those of C_{60}. We shall utilize this information in our attempt to arrive at the ultimate assignments in this paper.

The discovery of the conductivity[15] and superconductivity[16] of doped C_{60} and the existence of the polymeric fullerenes[17] have further stimulated the characterization of their vibrational properties. Originally, only doping in the form A_xC_{60} (A = K, Rb, or Cs) of the fullerene systems was investigated in detail. The phases with $x = 3$ were found to be metallic.[18] This metallic state occurs as a result of a partial filling of the first band (t_{1u}) above the Fermi level in the undoped material. Further doping yielded an insulating phase, A_6C_{60}. Raman and neutron scattering experiments[19] have shown that the charge transfer shifts

10.1021/jp991420h CCC: $19.00
Published on Web 12/09/1999

most of the Raman-allowed A_g and H_g bands to lower frequencies with a similar trend prevailing for the IR active F_{1u} modes as well.[20] In addition to the red shifts, a strong enhancement of the oscillator strength was observed with increasing doping. The enhancement was explained theoretically by a coupling of the additional carriers in the t_{1u}-derived conduction band to the F_{1u} modes by a virtual transition to the next highest t_{1g} band.[21] Understanding the details of polymerization or the mechanism of conductivity and superconductivity in these materials requires an analysis of the electron−phonon coupling strength.

Obviously, accurate theoretical prediction of these fundamental harmonic vibrational modes would greatly help in resolving the assignments. Considerable amount of theoretical work on the basis of various methods, such as classical spring mass model,[22] MNDO,[23] QCFF/PI,[24] force-constant model,[25] LDA,[26] and bond-charge-model,[27] was done to completely assign all fundamental modes of fullerene. However, these theoretical calculations were not sufficiently accurate to achieve conclusive vibrational assignments. A special challenge of the vibrational spectroscopy of fullerenes in general, and C_{60} in particular, is due to the strong coupling of the numerous internal coordinates in such highly fused ring systems. This aspect of the problem makes direct application of traditional force fields or traditional scaling techniques less accurate. To illustrate the problem, consider the fact that there are 90 CC bonds in C_{60}; consequently, out of the 174 total number of independent internal degrees of freedom, only 84 remain to be distributed over all angle bending and torsional degrees of freedom. This cannot be done in the traditional way. The alternative is to consider redundant coordinates,[28] as discussed in the next section.

Theoretical frequencies as obtained with ab initio Hartree−Fock (HF) are well-known to be consistently too high by about 10% or so[29] as compared with experiments due to the neglect of electron correlation and anharmonicity. In this regard, density functional theory (DFT), especially gradient-corrected exchange-correlation functionals, has been successfully applied in the direct predictions of vibrational properties.[30] However, even correlated methods such as DFT can be substantially improved by employing scaling procedures similar to the ones developed for scaling HF force fields.[31] Such procedures, other than uniform or exponential scaling, involve the transformation of the molecular force field (dynamic matrix) to chemically meaningful internal coordinates and the introduction of more than one scaling parameter for the various groups of internal coordinates. It is expected that the agreement of the frequencies scaled by multiple scaling factors as compared with experiment is better than if just a single uniform scaling factor is used. The transferability of scaling factors has also been demonstrated between rotational isomers[32] and between oligomers[33] of different size.

However, unless adopting symmetry coordinates, when it comes to the polycyclic systems such as fullerenes, it is extremely difficult if not impossible to uniquely define a set of chemically meaningful nonredundant internal coordinates. This problem has impeded the application of nonuniform scaling procedures to fullerenes. In this paper, we first demonstrate that the scaling procedure in redundant internal coordinates for the quantum chemical force field of fullerene and charged fulleride improves the agreements with experiment significantly, leading to reliable vibrational assignments for both. After that, the IR intensity enhancement of C_{60}^{6-} is analyzed.

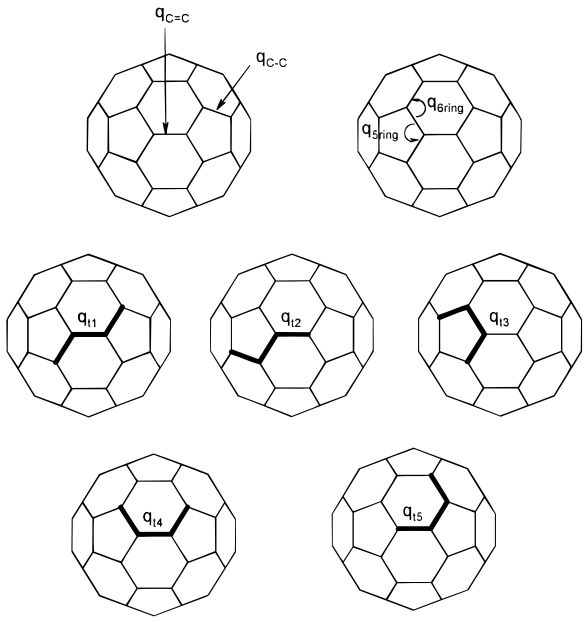

Figure 1. Nine unique valence internal coordinates in C_{60}.

Computational Details

Instead of constructing nonredundant internal coordinates, all primitive coordinates such as stretching, bending, and torsional modes were chosen, yielding 630 redundant internal coordinates.[28] These were used to construct the Wilsonian **B** matrix,[34] which transforms the internal displacement coordinates into Cartesian displacement coordinates. The generalized inverse[35] on the basis of singular value decomposition[36] method was used to obtain the **A** matrix, which is the generalized inverse of the **B** matrix. In C_{60}, there are nine unique primitive coordinates as shown in Figure 1. There are 30 single bond stretching type (q_{C-C}), 60 double bond stretching type ($q_{C=C}$), 60 five-membered ring bending type (q_{5ring}), 120 six-membered ring bending type (q_{6ring}), and 5 different types of 360 torsions (q_{t1} through q_{t5}), depending on the cis/trans position and the types of rings that are involved in the torsion: The torsions involved in q_{t1} and q_{t4} are around a bond at the edge of two 6-rings and the rest around a bond bordering a five- and a six-membered ring. The torsions correspond to infinitesimal torsions around the middle bonds highlighted in Figure 1. Once the quadratic Cartesian force constants are obtained with the quantum mechanical DFT calculation, they are transformed into redundant internal coordinates, then scaling is performed using these internal force constants, F_{ij} , according to[29]

$$F_{ij}^{\text{scaled}} = (s_i s_j)^{1/2} F_{ij} \qquad (1)$$

where s_i and s_j are scaling factors for the redundant internal coordinates i and j, respectively. These scaled force constants were then transformed back to Cartesian coordinates and a harmonic vibrational analysis was performed. It should be noted that due to strong couplings the typical values of the force constants in the redundant coordinates are far outside the usual range of force constants. The scaling factors were optimized by minimizing the root-mean-square deviations between the experimental and calculated scaled frequencies. Only the 14 unequivocally assigned (IR or Raman allowed) bands[2] were used in conjunction with the simplex method[36] in the scaling factor optimization. Due to the high symmetry of C_{60}, we chose two schemes, one with four and one with seven scaling factors. Attempts with the maximum number of scaling factors (9)

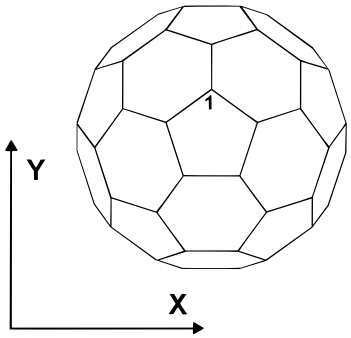

Figure 2. Orientation of C_{60} in the APT calculation.

yielded a smaller rms, but due to the relatively small number of experimental frequencies (14) the minimization resulted in an unphysical force field. In the C_{60}^{6-} case only a four-parameter minimization was performed due to the larger experimental uncertainties.[20c]

Full geometry optimization and the calculation of the unscaled dynamical matrix for pristine C_{60} and charged C_{60}^{6-} have been performed using ab initio Hartree−Fock and density functional theory[37] with the Becke (B)[38] and his three-parameter exchange functional (B3)[39] in combination with Lee−Yang−Parr (LYP)[40] correlation functionals and the STO-3G, 3-21G, and 6-31G* basis sets. All quantum mechanical calculations were performed with the Gaussian 94 program.[41]

The atomic polar tensors (APT)[42] determine the infrared intensities in the electric harmonic approximation and are defined as the dipole moment derivatives for the α-th atom

$$P_X^\alpha = \begin{pmatrix} \frac{\partial p_x}{\partial X_\alpha} & \frac{\partial p_x}{\partial Y_\alpha} & \frac{\partial p_x}{\partial Z_\alpha} \\ \frac{\partial p_y}{\partial X_\alpha} & \frac{\partial p_y}{\partial Y_\alpha} & \frac{\partial p_y}{\partial Z_\alpha} \\ \frac{\partial p_z}{\partial X_\alpha} & \frac{\partial p_z}{\partial Y_\alpha} & \frac{\partial p_z}{\partial Z_\alpha} \end{pmatrix} \quad (2)$$

where p_i is the ith component of the total molecular dipole moment. ($i = x, y, z$ and X_α, Y_α, Z_α, are the Cartesian coordinates of nucleus α.) These were also calculated with the Gaussian 94 program.[41] The molecular orientation is presented in Figure 2. Normal modes were studied using Visual Chem.[43]

No new experiments are reported here. The calculations are compared to a compilation of a wide range of published experimental data. For the IR and Raman spectra containing second-order combination and overtone modes, we used the selection rules discussed by Martin et al.[7] to determine the experimental fundamental frequencies.

It is essential to note that at the end of the fitting process all lines were successfully assigned to combination and overtone modes in both IR and Raman spectra in the region above 1570 cm^{-1}, the highest frequency fundamental. In several instances, more than one combination yields the same or nearly the same peak, however, *no peaks* remained *unassigned.* This provided a critical test in our reassignment, because a small change in the choice of the frequency of a fundamental always produces overtones that are sufficiently off to make the assignment unacceptable.

Results and Discussion

A. Structures of C_{60} and C_{60}^{6-}. Our HF and density functional calculations of C_{60} and C_{60}^{6-} using the HF/STO-3G, BLYP/3-21G, B3LYP/3-21G, and B3LYP/6-31G* methods are presented and compared with earlier calculations[44,45] and experiments[46,47] in Table 1. The MP2/TZP method[44e] shows the smallest bond length difference between the two unique bond lengths (see Figure 1) of C_{60}. We will refer to the shorter (a) bonds as C═C "double", and the longer (b) bonds as C−C "single" bonds, respectively. As compared to earlier local density functional calculations, our gradient-corrected density functional calculations yield slightly longer bond lengths for both types. The same trends can also be seen in the calculations for C_{60}^{6-}.

TABLE 1: Experimental and Theoretical Equilibrium Bond Distances of C_{60} and C_{60}^{6-}(in C)

	method	*a*	*b*	diameter	ref
C_{60}	QCFF/PI	1.411	1.471		44b
	HF/STO-3G	1.376	1.463		44a
	HF/tzp	1.370	1.448		44c
	LDA	1.382	1.444		44d
	MP2/TZP	1.406	1.446		44e
	LDA/DNP	1.391	1.444		26a
	DFPT	1.393	1.446		26b
	BLYP/3-21G	1.404	1.470	7.03	this work
	B3LYP/3-21G	1.390	1.460	6.97	this work
	B3LYP/6-31G*	1.395	1.454	6.96	this work
	exp (NMR)	1.40	1.45		46a
	exp (X-ray)	1.388(5)	1.432(9)		46b
C_{60}^{6-}	LDA	1.434	1.440		45a
	LDA	1.424	1.442		45b
	HF/STO-3G	1.430	1.444		this work
	B3LYP/3-21G	1.431	1.457	7.03	this work
	B3LYP/6-31G*	1.435	1.452	7.02	this work
	exp (neutron diff)	1.431	1.444		47

It is interesting that the length of the "double" bond of C_{60}^{6-} increases, while the length of the "single" bond decreases as compared to those of neutral species so as to yield a very small difference between the two bond lengths. According to our B3LYP/6-31G* calculations, this bond length difference is reduced from 0.06 Å in C_{60} to 0.02 Å in C_{60}^{6-}. This can be explained by the fact that the six extra electrons in C_{60}^{6-} fill up the full set of t_{1u} orbitals which have some π^* (antibonding) character and consequently increase the length of the C═C double bonds. Considering the 60 π electrons in C_{60}, the effect of extra 6 π electrons changes the bond length differences between the two types of bonds in C_{60} significantly. Bond equalization has been also observed in the DFT calculation for K_3C_{60} by Bohnen et al.[48] It might be worthwhile to note that HF generally underestimates the length of C═C bonds and overestimates the length of C−C bonds. This is the case for C_{60} as compared with correlated methods and experiments. On the other hand, HF predicts the bond distances of C_{60}^{6-} well. Judging from the success of the DFT geometries for both, it appears that the role of correlation is more important in the accurate description of localization/delocalization of π electrons in the "half-filled", i.e., neutral C_{60} case than in the charged species.

Zhou et al.[19d] have discussed the effect of the charge transfer on fullerene and argued that the expansion of the fullerene diameter leads a softening of the intraball force constants that determine the frequencies of the vibrational modes. According to our DFT calculations, however, the diameter of the fulleride increases as compared to that of the fullerene only by about 0.06 Å. It is expected, therefore, that the vibrational frequencies of C_{60}^{6-} will be strongly influenced by the bond equalization effect rather than the expansion of the ball.

B. Vibrational Properties of C_{60}. Representative earlier experimental and theoretical studies are collected in Tables 2 and 3, respectively. Both tables list in the last column our best

TABLE 2: Various Measured Vibrational Frequencies of C_{60} (in cm^{-1}) Compared with the Current Best Experimental Frequencies (Column O)[a]

	A	B	C	D	E	F	G	H	I	J	K	L	M	N	O
A_g	**498**	**495**			**496**	*488*		**493**					503	509	495
	1470	**1470**			**1467**		**1472**		**1467**						1470
F_{1g}	502	**563**		*535*		*673*		**563**	**566**				558	554	565
	976	973		1025		840						**908**			904
	1328	1479, 1484					1278								1290
F_{2g}	*667*	541		640				553				**613**			614
	865	764	**668**						**665**				**665**		668
	914	1214		**826**					**827**				838		831
	1360	1544		1503					**1342**						1340
G_g	**486**	**485**		*432*		**488**		**482**	**483**		504		**480**	468	485
	621	961		*611*				570	755			**753**	761	760	592
	806	1199		796											758
	1076	1330		*1166*			1028								1040
	1356	**1345**		*1470*			1359			*1310*			1368		1348
	1525	1596					1508		**1496**	*1525*					1497
H_g	273	**267, 272**	**270**	**270**	**272**	**271**		**265**	**265**	**262**	260				267
	433	**431**		**430**	485	**432**		**431**	**428**	437					431
	711	**709**		**707**	**709**	**715**			**708**	*668*					711
	775	**775, 778**	**778**	766	**772**	765			**771**	**776, 771**				**775**	775
	1101	**1102**		**1100**	**1100**	1089	1109		**1097**	1063			1093		1101
	1251	**1252**		**1250**	**1250**	1217	**1246**		**1248**	1265, 1272			1244		1251
	1427	1418, **1425**	**1425**	1443	**1424**	1563			**1427**	1477, *1468*					1427
	1578	1567, **1576**	**1576**	**1572**	**1574**		**1581**		**1572**	*1567*, **1573**					1576
A_u	*1143*	1122					1085		**1077**				**1082**		1078
F_{1u}	**527**	**526**				**526**		**528**	**525**		**525**		**526**, 517	**526**, 518	526
	579	**577**				563		**576**	**578**		**576**		**576**	**576**	577
	1183	**1183**				1217	1198		**1180**	1204			**1183**, 1192	**1183**, 1197	1180
	1429	**1429, 1433**	**1433**			1448	1440			**1433**					1433
F_{2u}	*356*	*353*		*354*				**343**	**339**		*351*				340
	680	**712**		*756*						**714**			724	722	716
	1026	*797*		*1037*					**960**				**960**		955
	1201	*1038*		1190						*1185*, 1172			**1145**	1130	1142
	1577	*1313*		*1566*			1532		**1524**	1606			**1527**		1524
G_u	*400*	*402*		*345*		344		**350**	**350**	**352**	*403*				354
	760	*739*		**712**		536				*797*			**705**		707
	924	*753*		*776*		813			**796**			**797**	816		797
	970	*1080*		963						961, 959					970
	1310	*1290*		1418			**1319**		1309	**1310, 1312**			**1313**		1315
	1446	*1526*		*1529*						**1426, 1425**					1429
H_u	*343*	*342*		**403**		264		**399**	**400**	**402**					403
	563	*579*		*485*		355		**535**	**532**	**536**			542	542	535
	696	*664*, *668*		*667*		*404*				743, *737*			**689**, 682		694
	801	*827*		**738**		576			**739**	832, 841			**742**	**749**	737
	1117	1222		**1215**					**1211**	**1216**					1214
	1385	1242		1503						**1342, 1338**					1343
	1559	1600		1540					**1572**	**1567**, *1573*			1556		1567

[a] Columns A−N are defined and discussed in the text. Column O is our assignment. Bold characters indicate agreement with the present assignment (within ±5 cm^{-1}). Italics are similar numerical agreement, except the frequency has to be assigned to a different mode, as indicated in the text.

assigned frequencies. Before discussing the spectra in some detail, we first summarize column by column the major disagreements with respect to the current best frequencies listed in Table 2. (A color-coded illustration of the frequencies of Tables 2 and 3 is given in Figure 3, which should aid the comparison.)

A. Raman study by Wang et al. (1993).[7] We have reassigned the following frequencies: 667 F2g(2), 1076 Au, 1525 F2u(5), 1143 F2u(4), 356 Gu(1), 1577 Hg(8), 400 Hu(1), 760 Gg(3), 343 F2u(1), 563 F1g(1), 801 Gu(3) cm^{-1}.

B. IR transmission study by Martin et al. (1994).[8] We have reassigned the following frequencies: 973 Gu(4), 1214 Hu(5), 353 Gu(1), 797 Gu(3), 1038 Gg(4), 1313 Gu(5), 402 Hu(1), 739 Hu(4), 753 Gg(3), 1080 Au, 1290 F1g(3), 1526 F2u(5), 342 F2u(1), 579 F1u(2), 664 and 668 F2g(2), 827 F2g(3) cm^{-1}.

C. Electron energy loss spectroscopy results by Gensterblum et al. (1991).[5a] We have determined the numbers form the published graphs; however, all mode assignments are ours.

D. IR spectra of labeled C60 by Cardini et al.[6] We have reassigned the following frequencies: 535 Hu(2), 1503 Gg(6), 432 Hg(2), 611 F2g(1), 1166 Gu(3), 1470 Ag(2), 354 Gu(1), 756 Gg(3), 1037 Gg(4), 1566 Hu(8), 345 F2u(1), 776 Hg(4), 1529 F2u(5), 485 Gg(1), 667 F2g(2) cm^{-1}.

E. FT-Raman study by K. Lynch et al. (1995).[3a]

F. Neutron scattering study by Coulombeau et al. (1992).[2g] We have reassigned the following frequencies: 488 Gg(1), 673 F2g(2), 1217 Hu(5), 1563 Hu(7), 563 F1g(1), 1217 Hu(5), 344 F2u(1), 776 Hg(4), 1529 F2u(5), 485 Gg(1), 667 F2g(2) cm^{-1}.

G. High-resolution neutron scattering results by Coulombeau et al.[49] All lines are close to assigned frequencies, but outside of the 5 cm^{-1} limit.

H. Heid et al.[11] The 553, 563, 570, and 576 cm^{-1} lines were resolved from a single peak around 70 meV. We cannot assign the 553 and 570 cm^{-1} bands.

I. Photoluminscence spectroscopy by Nissen et al. (1992).[10] The measured frequencies were not assigned by the authors. We made an assignment whenever it was compatible with ours. We could not assign the 1270 cm^{-1} band.

J. First number: Sassara et al. (1996)[12a] fluorescence in rare gas matrices. Second number: Sassara et al. (1996)[12b] phos-

TABLE 3: Calculated Vibrational Modes of C_{60} (in cm^{-1}) Compared with the Current Best Experimental Frequencies (Column O)[a]

	P[44b]	Q[26c]	R[25]	S[48]	T[26b]	U[26a]	V	O
A_g	513	478	**492**	481	**495**	483	484	495
	1442	1499	**1468**	1489	1504	1529	**1474**	1470
F_{1g}	597	580	501	**563**	**564**	**566**	556	565
	975	788	981	826	823	825	896	904
	1398	1252	1346	1241	1296	**1292**	**1295**	1290
F_{2g}	637	547	541	543	548	550	608	614
	834	610	847	788	767	771	683	668
	890	770	931	800	794	795	**836**	831
	1470	1316	1351	1277	1363	1360	**1340**	1340
G_g	476	**486**	498	**480**	**480**	**484**	493	485
	614	571	626	570	566	564	605	592
	770	**759**	805	772	**762**	**763**	721	758
	1158	1087	1056	**1037**	1118	1117	1054	1040
	1450	1296	1375	1287	1322	1326	1342	1348
	1585	1505	1521	**1501**	1512	1528	**1498**	1497
H_g	258	258	**269**	**263**	259	**263**	**272**	267
	440	439	439	422	425	**432**	**436**	431
	691	**712**	**708**	717	**711**	**713**	704	711
	801	767	788	763	783	**778**	782	775
	1154	1093	**1102**	1080	1120	**1111**	1117	1101
	1265	1244	1217	1198	1281	1282	**1250**	1251
	1465	1443	1401	**1422**	1450	1469	1419	1427
	1644	**1576**	**1575**	**1580**	**1578**	1598	1582	1576
A_u	1206	850	1142	973	943	947	1064	1078
F_{1u}	544	547	505	514	**527**	533	520	526
	637	570	589	569	586	548	**576**	577
	1212	**1176**	1208	1143	1218	1214	1172	1180
	1437	1461	1450	1457	1462	1485	**1430**	1433
F_{2u}	350	**342**	367	**343**	**337**	**344**	347	340
	690	738	677	725	**716**	**717**	707	716
	999	962	1025	945	993	987	**956**	955
	1241	1185	1212	1131	1228	1227	**1144**	1142
	1558	1539	1575	1546	1535	1558	1543	1524
G_u	**358**	**356**	385	348	**349**	**356**	365	354
	816	683	789	756	748	752	700	707
	832	742	929	790	782	784	**798**	797
	1007	957	961	937	**975**	977	**973**	970
	1401	1298	1327	1259	1334	1339	1306	1315
	1546	1440	1413	1420	1452	1467	**1424**	1429
H_u	**403**	**404**	361	388	**399**	**406**	425	403
	531	**539**	543	527	**530**	**534**	542	535
	724	657	700	661	662	663	702	694
	812	**737**	801	750	**741**	**742**	**742**	737
	1269	1205	1129	1176	1231	1230	1242	1214
	1469	1320	1385	1291	1363	1360	1358	1343
	1646	**1565**	1552	**1566**	**1569**	1588	1560	1567

[a] Columns P−U are literature values as defined and discussed in the text, V contains our calculated values, the experimental data are in column O (the same as in Table 2). Bold characters mean agreement with the present assignment within ±5 cm^{-1}.

phorescence. We reassigned the following bands: 1310 Gu(5), 1525 F2u(5), 668 F2g(2), 1468 Ag(2), 1567 Hu(7), 1185 F1u-(3), 797 Gu(3), 959 F2u(3), 737 Hu(4), 832 F2g(3) cm^{-1}.

K. Long et al. (1998).[14] IR on labeled C_{60}^- monoanion. Measured frequencies may be shifted due to charge state. Reassigned: 351 Gu(1), 403 Hu(1) cm^{-1}.

L. Martin et al. (1994)[8] (same as in A). Pressure polymerized C_{60}. Only the new lines, produced by the pressure treatment, are listed. Mode assignment is ours.

M. Mihaly et al.,[13] IR spectra of polymerized C_{60}^-. Measured frequencies may be shifted due to charge state. Mode assignment is ours.

N. Mihaly et al.,[13] IR spectra of dimerized C_{60}^-. Measured frequencies may be shifted due to charge state. Mode assignment is ours.

While Coulombeau et al.[2g] reported only 23 peaks out of 46 expected bands on the basis of neutron inelastic spectroscopy showing the overlaps of many peaks and the effect of the instrumental resolution, Martin et al.[7] observed approximately 150 bands in the IR transmission spectrum of large C_{60} crystals. As discussed in the Introduction, the origin of these peaks may be due to crystal field effects, combination bands, overtones, rotational perturbations, or even impurities. Model calculations were used in assigning the bands in several earlier works. Some representative calculations are summarized in Table 3 and compared with the current best experimental frequencies (last column, O). The QCFF/PI[44b] model (column P) overestimates the frequencies of most of the bands, but worse than that, some bands are completely misplaced. Other semiempirical calculations (columns Q and R) are also qualitatively correct at best. The LDA[26] calculations (columns Q, T and U) faithfully reproduce many bands especially in the low-frequency region, but are still not accurate enough to reliably assign most of the bands. The ab initio calculation of Bohnen et al.[48] (column S) is similar in some respects to ours (column V), but due to the more sophisticated scaling ours is much more reliable. While the assignments of the optically active 14 bands are in good agreement among different experiments and the LDA calculations, there are many points of disagreement concerning the silent modes.

Selection of reliable experimental frequencies to be used in the rms minimization is very important in the scaling procedure. In the case of C_{60}, since the optically active modes should be most reliable, only these 14 frequencies were used in this study for determining the scaling factors. (Concerning the controversial 430 cm^{-1} mode,[3] we accepted the revised assignment of Gallagher et al.[4]) Since such a small number of reference frequencies may yield unphysical scaled force constants, the number of scaling factors was originally reduced to 4 and then increased to 7, carefully watching the changes of each predicted frequency. Furthermore, vibrational calculations were done with both BLYP/3-21G and B3LY/3-21G methods to increase the reliability of the scaling procedure. The final scaling factors are presented in Table 4. (Table S1 of the Supporting Information contains a detailed comparison of the six different scaled and unscaled calculations.) The scaling factor for the q_{5ring} coordinate is somewhat smaller than other scaling factors. No scaling factor deviates too much from 1.0. The agreement of the scaled frequencies between the BLYP and the B3LYP results as compared with experiment for the optically active modes is significantly improved even with 4 scaling factors showing 9.7 and 8.3 cm^{-1} rms, respectively. With 7 scaling factors, the agreement further improves yielding 8.9 and 7.1 cm^{-1} rms, respectively. The improvement of scaled frequencies with 7 scaling parameters over with 4 parameters is modest indicating that the scaling procedure is more or less converged within this scaling scheme. The discrepancy in predicted frequencies between the two methods is significantly reduced after the scaling further showing the stability of our scaling procedure.

The available experimental data is summarized in Table 2 and illustrated in Figure 3 (left-hand side). In most of the experiments it is much easier to determine the vibrational frequency than the symmetry assignment. Indeed, many of the experimental frequencies coincide, whereas the mode is assigned differently. On the other hand, the different experimental conditions may lead to somewhat different mode frequency. For example, some measurements were performed at room temperature, whereas others at low temperatures; sometimes the fullerene molecules were embedded in a matrix; in more extreme cases the fullerene molecules were chemically modified, doped, or polymerized. Therefore, we picked the "best experimental"

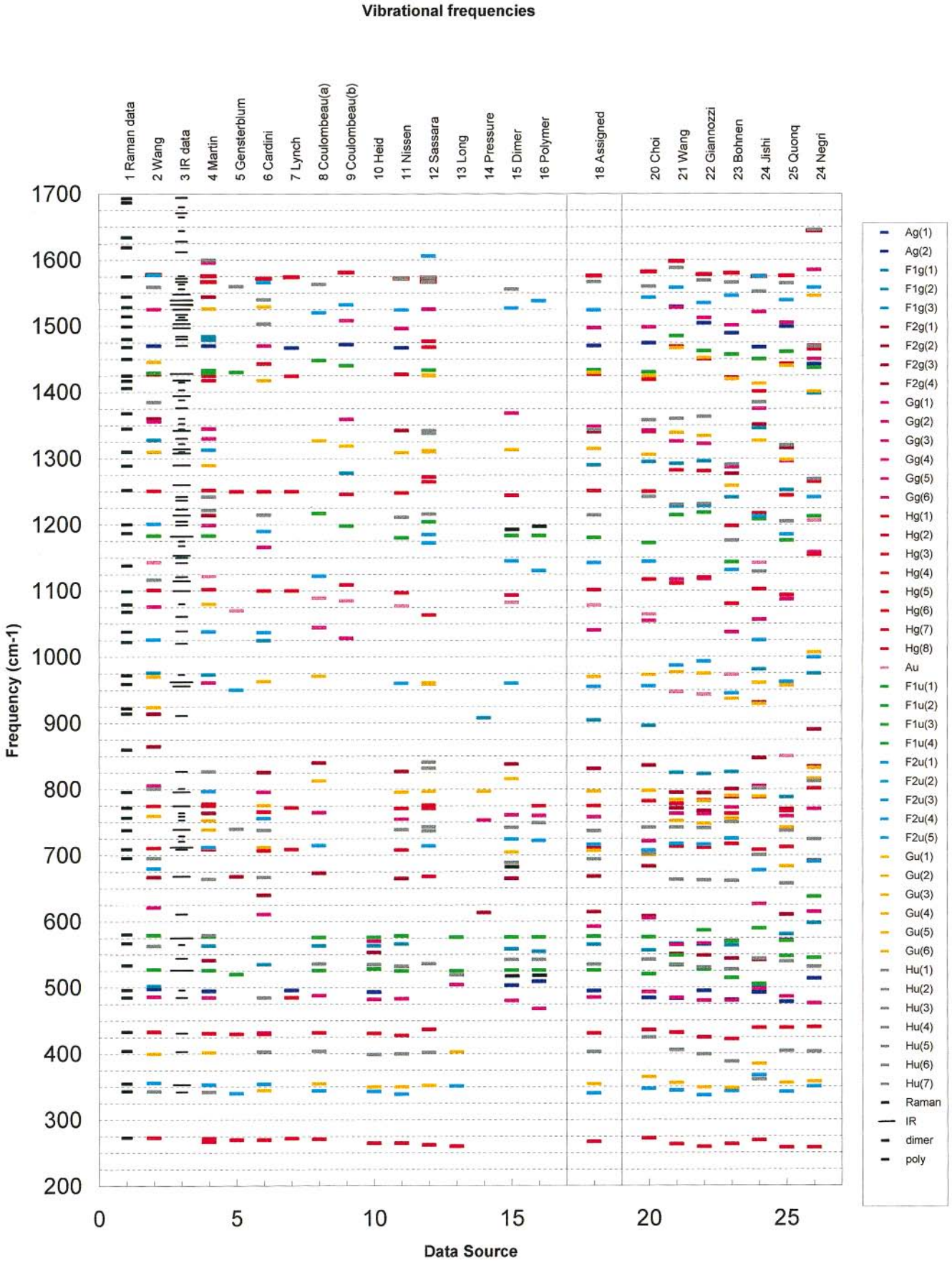

Figure 3. Vibrational frequencies sorted by symmetry species, each indicated by different colors. Columns 1−16 are experimental data, columns 20−24 are theoretical values, and column 18 is the best assigned experimental set of frequencies.

frequency so that it overlapped with as many measurements as possible. Naturally, a larger margin was allowed for neutron scattering, where the uncertainty of the frequency is larger, than for the optical methods, where the frequencies are more accurate.

TABLE 4: Optimized Scaling Factors[a]

	C_{60}				C_{60}^{6-}
	BLYP		B3LYP		B3LYP
	4 param	7 param	4 param	7 param	4 param
$q_{C=C}$	1.056	1.028	0.965	0.974	1.026
q_{C-C}		1.072		0.963	
q_{5ring}	0.833	0.849	0.811	0.825	0.772
q_{6ring}	1.256	1.263	1.145	1.119	1.191
q_{t1}	1.174	1.131	1.072	1.093	1.257
q_{t2}	1.174	1.099	1.072	0.990	1.257
q_{t3}	1.174	1.247	1.072	1.129	1.257
q_{t4}	1.174	1.247	1.072	1.129	1.257
q_{t5}	1.174	1.247	1.072	1.129	1.257
rms (cm^{-1})	9.7	8.9	8.3	7.1	15.0

[a] Internal coordinates are defined in Figure 1.

New lines appearing in the IR spectrum of fullerene compounds, dimers, and polymers were used as an indicator for a fundamental mode in the neighborhood of that line (assuming that the primary effect of the symmetry breaking is making the line IR active, whereas the line frequency may also shift somewhat). Once the frequency of the mode is picked, we searched for a close calculated frequency, and used it for symmetry assignment. The remaining ambiguities were resolved by looking at the combination modes in the IR and Raman data, including frequencies up to 3000cm^{-1}.

In the 200 cm^{-1} region, two peaks at 264 and 271 cm^{-1} were observed by the NIS in solid C_{60} at 25 K and assigned as H_u and H_g, respectively. Two peaks at 266 and 272 cm^{-1} in crystalline C_{60}, and one peak at 265 cm^{-1} in C_{60}/CS_2 solution, were also reported by FTR.[3] However, Lynch et al.[3] assigned only the peak at 272 cm^{-1} in crystalline C_{60} to H_g symmetry arguing that the peak at 266 cm^{-1} in crystalline is due to "solvated C_{60}". Martin et al.[7] reported two peaks at 267 and 272 cm^{-1} in C_{60} crystal, but treated them as corresponding to the same set of fundamental H_g modes. According to our results, only one peak, 272 cm^{-1}, is calculated to be in 200 cm^{-1} region and assigned as H_g. Since two peaks were observed only in crystalline C_{60}, the origin of the two peaks in 200 cm^{-1} should be attributed to the crystal field effect rather than to the "solvated C_{60}". We question the assignment of the 264 cm^{-1} peak (NIS)[2g] and agree with the assignment of this band by Martin et al.[7]

In the 300 cm^{-1} region, two peaks at 344 and 355 cm^{-1} were observed by NIS and assigned as G and H_u, respectively. The fact that, while the corresponding two peaks were observed by IRT, they were not observed by FTR, showing that these two peaks should have ungerade symmetry. Martin et al.[7] assigned them as H_u and F_{2u}, respectively. Cardini et al.[14] observed the corresponding peaks at 345 and 354 cm^{-1} and assigned them as G_u and F_{2u}. However, their assignments were based on earlier semiempirical calculations[44b,50] which should be inferior to our SQM results. Our SQM yields two sets of modes at 347 (F_{2u}) and 365 (G_u) cm^{-1} in this region. Although the frequency difference between the two peaks is small, the fact that the same order can be found in our unscaled results and earlier LDA results[26b] further supports our assignment. It is interesting to note that our assignment can be brought into agreement with Wang et al. [6] and Martin et al.,[7] if the orders of the lowest F_{2u}, G_u, and H_u bands are adjusted accordingly.

In the 400 cm^{-1} region, three peaks 404, 432, and 488 cm^{-1} were observed by NIS. Since the peaks at 404 and 488 cm^{-1} were intense, Coulombeau et al.[2g] suggested that they result from the overlap of more than one bands. Martin et al.[7] reported four peaks at 402, 431, 485, and 495 cm^{-1} and assigned them as G_u, H_g, G_g, and A_g in this region. Lynch et al.[3] reported peaks at 430, 435, 485, and 495 cm^{-1}, but as mentioned in the Introduction, they did not consider the peaks at 430 and 435 cm^{-1} as fundamentals. Instead, they assigned the 485 and 495 cm^{-1} bands as H_g and A_g, respectively. Our SQM yielded normal modes at 425, 436, 484, and 493 cm^{-1}, and we assigned the experimentally found peaks at 403, 431, 485, and 495 cm^{-1} as H_u, H_g, G_g, and A_g, respectively. The frequency of our calculated peak at 425 cm^{-1} is somewhat overestimated.

In the 500 cm^{-1} region, four peaks at 526 (F_{1u}), 536 (G), 563 (F_{1u}), and 576 (H_u) cm^{-1} were observed by NIS. Martin et al.[7] reported peaks at 526 (F_{1u}), 541 (F_{2g}), 568 (F_{1g}), 577 (F_{1u}), and 579 (H_u) cm^{-1}. Lynch et al.[3] reported peaks at 509, 535, and 568 cm^{-1} but did not assign them as fundamentals. Our best SQM yielded normal modes at 520, 542, 556, and 576 cm^{-1} as F_{1u}, H_u, F_{1g}, and F_{1u}, respectively. As Martin et al.[7] have shown, the IR active peaks at 526 and 577 cm^{-1} are so strong that they saturate with zero transmission, and the peak at 579 cm^{-1} could not be observed accurately. In this regard, although the resolution is low, NIS results should be more reliable and are well reproduced by our SQM results.

In the 600 cm^{-1} region, only one peak at 673 cm^{-1} was observed by NIS. Martin et al.[7] reported also only one peak at 668 cm^{-1} as H_u. Raman study by Lynch et al.[3] did not indicate any peak around this region. Interestingly, earlier IR study by Wang et al.[6] showed peaks at 621, 667, 680, and 696 cm^{-1} and were assigned as G_g, F_{2g}, F_{2u}, and H_u, respectively. Cardini et al.[14] also reported peaks at 611 (G_g), 640 (F_{2g}), and 667(H_u). In fact, Martin et al.[7] observed a strongly pressure dependent peak at 611 cm^{-1}, but they assigned it as a combination band. Strong pressure or temperature dependence may be indicative of fundamentals (the anharmonicity of the internal molecular vibrations is not expected to be very sensitive to the environment, and therefore combination modes should not be strongly pressure or temperature dependent). Our SQM yielded normal modes at 605 (G_g), 608 (F_{2g}), 683 (F_{2g}), and 700 cm^{-1} (G_u) with 7 scaling parameters, using B3LYP. On the basis of these results, we propose that observed peaks at 611 cm^{-1} is actually the F_{2g} fundamental, whereas the peaks at 670 and 695 cm^{-1} are assigned to a H_g+H_u combination and a G_u species, respectively.

In the 700−900 cm^{-1} region, the IR data exhibit many, closely packed features, with characteristic sharpening in the temperature dependence (Figure 5). The NIS showed four peaks at 715 (H_g), 765 cm^{-1} (H_g), 813 (F), and 840 (F). However, they also suggested that the broad band at 765 should be composed of three to five peaks. Lynch et al.[3] reported peaks only at 709 (H_g), 754, and 772 (H_g) cm^{-1}. Cardini et al.[14] reported also 8 peaks at 707 (H_g), 712 (G_u), 738 (H_u), 756 (G_u), 766 (G_g), 776 (G_u), 796 (G_g), and 826 (F_{2g}) cm^{-1}. SQM yielded 9 sets of degenerate normal modes at 702 (H_u), 704 (H_g), 707 (F_{2u}), 721 (G_g), 742 (H_u), 782 (H_g), 798 (G_u), 836 (F_{2g}), and 896 (F_{1g}) cm^{-1}. The two H_g sets (around 710 and 780 cm^{-1}) in this region can be reliably assigned, since they are Raman active. Our results shows that there are more than two fundamental symmetry species around 700−720 cm^{-1}. The calculated peak at 896 (F_{1g}) cm^{-1} might be the one observed at 911 cm^{-1} by Martin et al. who assigned it as a combination band. The observed peaks at 840 cm^{-1} by NIS are well reproduced by our SQM at 836 (F_{2g}) cm^{-1}. However, the other NIS band at 813 (F) cm^{-1} probably corresponds to the band observed in the IRT at 797 (F_{2u}) cm^{-1} which is in agreement with our SQM at 798 (G_u) cm^{-1}.

In the 900−1200 cm^{-1} region, four peaks at 971 (F+G), 1044, 1089 (H_g), and 1120 (F) cm^{-1} were observed by NIS.

Martin et al.[7] reported peaks at 961 (G_g), 973 (F_{1g}), 1038 (F_{2u}), 1080 (G_u), 1102 (H_g), 1122 (A_u), 1183 (F_{1u}), and 1199 (G_g) cm^{-1}. Lynch et al. reported peaks at 1067, 1078, 1100 (H_g), and 1110 cm^{-1}. Cardini et al. reported peaks at 963 (G_u), 1025 (F_{1g}), 1037 (F_{2u}), 1100 (H_g), 1166 (G_g), and 1190 (F_{2u}) cm^{-1}. Although the symmetry assignments are different, SQM yielded fundamental frequencies at 956 (F_{2u}), 973 (G_u), 1054 (G_g), 1064 (A_u), 1117 (H_g), 1144 (F_{2u}), and 1172 (F_{1u}) cm^{-1} which reproduced most of peaks (see Figure 3) except the peak at 1199 cm^{-1}. According to our results in this region, there should be only one peak between 1166 and 1200 cm^{-1}. The experimental peaks at 1080 and 1122 cm^{-1} are combination bands, and our predicted normal modes at 1064 and 1144 cm^{-1} probably correspond to the experimental peaks at 1068 and 1142 cm^{-1}, respectively.

In the 1200−1400 cm^{-1} region, peaks at 1217, 1327 cm^{-1} were observed by Coulombeau et al. (NIS),[2g] who suggested that, since these peaks were so intense, these may be degenerate modes that are associated with each of these two bands. Martin et al. reported peaks at 1214 (F_{2g}), 1222 (H_u), 1242 (H_u), 1252 (H_g), 1290 (G_u), 1313 (F_{2u}), 1330 (G_g), and 1345 (G_g) cm^{-1}. Lynch et al. reported peaks at 1244 and 1250 (H_g) cm^{-1}. SQM yielded normal modes at 1242 (H_u), 1250 (H_g), 1295 (F_{1g}), 1306 (G_u), 1340 (F_{2g}), 1342 (G_g), and 1358 (H_u) cm^{-1}. According to our results, the peaks at 1214 and 1222 cm^{-1} observed by Martin et al. should not be assigned as fundamentals. They also observed a peak at 1368 cm^{-1} but assigned it as a combination band. However, Wang et al.[6] assigned it as a G_g fundamental at 1356 cm^{-1}, very close to the 1358 (H_u) cm^{-1} SQM frequency. Except these three bands, our SQM results very well reproduced the peaks found by Martin et al.[7] The strongly temperature-dependent peak at 1319 cm^{-1} (Figure 5) is due to a set of G_u modes.

In the 1400−1600 cm^{-1} region, peaks at 1520, 1563 (H_g), 1603, and 1702 cm^{-1} were found by NIS. Martin et al.[7] reported peaks at 1418+1425 (H_g), 1429+1433 (F_{1u}), 1470 (A_g), 1479+1484 (F_{1g}), 1526 (G_u), 1544 (F_{2g}), 1567+1576 (H_g), 1596 (G_g), and 1600 (H_u) cm^{-1}. Lynch et al. reported 15 peaks in this region. SQM yielded normal modes at 1419 (H_g), 1424 (G_u), 1430 (F_{1u}), 1474 (A_g), 1498 (G_g), 1543 (F_{2u}), 1560 (H_u), and 1582 (H_g) cm^{-1}. Martin et al. assigned the two peaks at 1418 and 1425 cm^{-1} to the same H_g fundamental. However, our corresponding results at 1419 and 1424 cm^{-1} clearly show that these are really two different fundamentals. Our predicted modes at 1430, 1474, 1543, and 1560 cm^{-1} well reproduced the peaks at 1429+1433, 1479, 1544, and 1567 cm^{-1} observed by Martin et al. However, our SQM could not reproduced the peak at 1526 cm^{-1} of Martin et al. but rather yielded a peak at 1498 (G_g) cm^{-1}. In fact, Martin et al. observed a peak at 1497 cm^{-1} but assigned it as a combination band. We suggest that this should be considered as a fundamental while the peak at 1526 cm^{-1} should not. Martin et al. assigned the two peaks at 1567 and 1576 cm^{-1} to the same H_g fundamental. However, we suggest that these should be assigned as sets of H_u and H_g fundamental modes, with the H_u exhibiting a particularly strong temperature dependence. Our results did not yield any peaks above 1582 cm^{-1} nor did other experiments. Therefore, no peak significantly above 1580 cm^{-1} should be assigned as a fundamental mode. Table 3 summarizes the new assignments and compares them with our best theoretical predictions. The rms value of 11.1 cm^{-1} small albeit somewhat larger than the value of 7.1 cm^{-1} that was obtained for the same calculation using only the 14 allowed bands. This high quality of fit indicates that an even and unbiased force field was obtained by the SQM method.

The frequency shifts predicted for the $^{12}C_{59}13C_1$ isotopomer indicate that there are only three bands that are shifted significantly (in cm^{-1}). Relative to the values in Column V of Table 3 are 1419 (H_g) by −6; 700 (G_u) by −5, and 1242 (H_u) by −5.

The breaking of the symmetry due to the single ^{13}C isotope substitution makes many silent modes slightly allowed. Martin et al.[8] found in a molecular dynamics simulation that the intensity gains due to this symmetry breaking is very small. Our calculation on the isotope substituted fullerene confirmed this finding with one exception: none of the bands acquires any significant IR intensity due to this symmetry breaking except one H_g derived band at 1413 cm^{-1}. The calculated intensity for this band is 0.9 km/mol or about 10% of the calculated intensities of the weaker F_{1u} allowed bands, which should make this band observable. Unfortunately, this 1413 cm^{-1} band is being masked by the nearby allowed F_{1u} band at 1429 cm^{-1} that has a calculated intensity of 13 km/mol. The intensity ratios of the four IR-allowed bands agree with experiment within the experimental error, as will be discussed in the last section in connection with the intensity enhancement due to charge transfer.

Although there are uncertainties in the experiments, it seems that the force field based on the scaled B3LYP/3-21G method yields a consistent assignment for all silent modes. Therefore, extension to the vibrational study to charged C_{60} is well warranted.

C. Vibrational Properties of C_{60}^{6-}. The experimental and theoretical vibrational frequencies of C_{60}^{6-} are presented in Table 5, where the last column indicates calculated neutral C_{60} vibrational frequencies. Force field scaling was also applied to this charged system. However, the fit is not as good as for the neutral molecule yielding a 15 cm^{-1} rms value using 4 scaling factors, which are listed in Table 4. Due to the large intensities, the positions of the four IR-active bands carry large experimental errors that may artificially increase the rms value and hinder further refinement of the scale factor optimization. Furthermore, the observed frequencies depend somewhat on the nature of the countercations[19,20] and also undergo solid state (Davydov) splitting, which are influencing factors that molecular calculations such as the ones discussed here cannot take into account.

The observed overall red shifts of the peaks[20,25] have been reproduced by our calculations. Comparison with experiment is complicated by splittings as reported by Zhou et al.[19d] One of our main objection to earlier assignments based on these splittings is, that in some cases the observed splitting was as large as 30 cm^{-1} and in other cases, no splitting was observed. Therefore, an alternative analysis is offered by considering that some Raman inactive modes become active by lowering the symmetry. The peaks at 1094 and 1120 cm^{-1} could be assigned as the calculated peaks at 1080 (A_u) and 1132 cm^{-1} (H_g). Similarly, the experimentally found peaks at 270 and 281 cm^{-1} could be assigned to the H_g species, but they can also be interpreted as H_u and H_g. The peaks at 420 and 427 cm^{-1} are likely to arise from the splitting of the H_g mode as suggested by Zhou et al.[19d] Finally the peaks at 656 and 676 cm^{-1} may be assigned as F_{2g} or F_{2u} and H_g modes.

Due to a large IR intensity enhancement[25,26] in charged C_{60}, accurate measurements of the peak positions is not trivial. Pichler et al.[20b] have adopted IR reflectivity measurements in combination with a quantitative line shape analysis and reported peak positions of the IR active F_{1u} bands (see Table 5). Our scaled frequencies are consistent with the experiments showing

TABLE 5: Experimental and Theoretical Vibrational Frequencies As Calculated with the 3-21G Basis Set of C_{60}^{6-} (in cm^{-1})

	K_6C_{60}	B3LYP		neutral C_{60}B3LYP
	exp[a]	unscaled	scaled w/4 param	w/7 param[b]
A_g	502	477	482	484
	1432	1414	1430	1474
F_{1g}		473	532	556
		833	907	896
		1264	1322	1295
F_{2g}		545	599	608
		576	645	683
		828	854	836
		1303	1360	1340
G_g		438	487	493
		532	594	605
		585	620	721
		1108	1134	1054
		1303	1340	1342
		1444	1482	1498
H_g	270, 281	258	277	272
	420, 427	400	443	436
	656, 676	591	658	704
	762	753	791	782
	1094, 1120	1090	1132	1117
	1237	1192	1236	1250
	1384	1346	1372	1419
	1476	1473	1493	1582
A_u		970	1080	1064
F_{1u}	467	410	460	520
	564	556	577	576
	1183	1159	1184	1172
	1341	1304	1318	1430
F_{2u}		345	372	347
		578	646	707
		988	1014	956
		1153	1167	1144
		1443	1458	1543
G_u		329	366	365
		473	531	700
		774	810	798
		938	968	973
		1284	1311	1305
		1378	1433	1424
H_u		257	268	425
		434	482	542
		493	557	702
		682	743	742
		1051	1138	1242
		1289	1320	1358
		1401	1432	1560

[a] IR data are taken from ref 20b and Raman data are taken from ref 19d. [b] From Table 3, column V.

red shifts except for the 1183 cm^{-1} peak. The assignment of the silent modes awaits further experimental tests.

D. IR Intensities of C_{60} and C_{60}^{6-}. Calculated IR intensities are summarized in Table 6. The observed intensities of the four F_{1u} modes are reproduced by the calculations beyond expectations, lending further credibility to the SQM method. The considerable enhancement upon charge transfer of the IR intensity of the $F_{1u}(2)$ and $F_{1u}(4)$ bands is also predicted in remarkable agreement with the experiment. The calculated enhancement for the $F_{1u}(3)$ is too small but qualitatively in agreement with the experiment. However, for the $F_{1u}(1)$ mode theory predicts a reduction of intensity rather than an enhancement. It is interesting to note[20b,c] that experimentally the most reliable are the $F_{1u}(2)$ and $F_{1u}(4)$ bands. The other two bands are less certain,[20b,c] and a reduction of intensity was observed for the $F_{1u}(1)$ band for small a value of charge transfer ($x = 1$, in A_xC_{60}). Nevertheless, it seems that the present molecular calculations can reproduce most of the intensity enhancement upon charge transfer.

TABLE 6: Theoretical IR Intensities (I) of C_{60} and C_{60}^{6-} in km/mol[a]

	C_{60}			C_{60}^{6-}		
		rel intensity			intensity ratio	
	I	theory[b]	exp[c]	I	theory[d]	exp[e]
$F_{1u}(1)$	28.5 (526)	100	100	8.7 (467)	0.3	1.5
$F_{1u}(2)$	7.3 (577)	26	27	178.0 (564)	24	20
$F_{1u}(3)$	8.8 (1183)	31	30	62.5 (1183)	7.1	2.5
$F_{1u}(4)$	13.1 (1433)	46	40	706.2 (1341)	54	73

[a] Numbers in parentheses are the corresponding experimental frequencies, theoretical values were obtained with scaled B3LYP/3-21G. [b] Calculated relative intensities. [c] Experimental relative intensities taken from ref 20b. [d] Calculated intensity ratio for C_{60}^{6-}/C_{60}. [e] Experimental intensity ratio for C_{60}^{6-}/C_{60} taken from ref 20b.

TABLE 7: Atomic Polar Tensor of Atom 1 of C_{60} and C_{60}^{6-} As Calculated with Scaled B3LYP/3-21G (in e)[a]

C_{60}			C_{60}^{6-}		
0.087	0	0	−0.104	0	0
0	0.035	0.075	0	0.301	0.407
0	0.078	−0.123	0	−0.323	−0.497

[a] The orientation of atom 1 is presented in Figure 2.

The large enhancement of the IR intensity of the $F_{1u}(2)$, $F_{1u}(3)$, and $F_{1u}(4)$ peaks can be explained by the enhancement of the atomic polar tensor (APT). The degenerate normal modes corresponding to the $F_{1u}(4)$ band are combinations of the five-membered rings expanding at one side of C_{60} (say the "north pole") and shrinking at the opposite side ("south pole"), the C═C "double" bonds are also expanding and shrinking. Due to the charge transfer in C_{60}^{6-}, the double bond character is reduced dramatically. This fact is illustrated by the calculated APT of C_{60} and C_{60}^{6-} as presented in Table 7. (APT of all other atoms can be deduced from that of atom 1 by tensor rotations.) The *YY* component, which lies in the C═C stretching direction, is about 10 times larger in the charged fullerene. Furthermore, the *YZ* and *ZY* components also show large increases. The large IR intensity enhancement of the $F_{1u}(2)$ band is also related to the changes of the APT. The normal modes belonging to this species can be described by the five-membered rings moving inward and outward on the opposite poles, accompanied again by C═C double bond stretching. In this case, the normal modes are more closely related with the *YZ* and *ZY* components of APT. Therefore, its enhancement is not as large as that of the $F_{1u}(4)$ band. We conclude that a large part of the IR intensity enhancement upon doping is a molecular effect rather than solid state phenomenon, in agreement with the analysis of Rice and Choi.[21]

Conclusions

DFT vibrational calculations in combination with force field scaling in fully redundant internal coordinates of C_{60} and C_{60}^{6-} have been performed in order to obtain reliable fundamentals of C_{60} and to study the effect of charge transfer on the vibrational spectrum of C_{60}^{6-}. Our results are in excellent agreement with the experiments and yield reliable assignments for the silent modes. We have also demonstrated that the force field scaling of C_{60}, which poses a serious challenge for traditional force constant scaling schemes, is feasible in fully redundant internal coordinates. The calculated intensity ratios for the IR allowed bands are in excellent agreement with the experiment.

The remarkable enhancement of IR-active $F_{1u}(2)$ and $F_{1u}(4)$ bands in C_{60}^{6-} can be to a large degree explained by the enhancements of certain components of APT partially due to the bond equalization of the charged system without reference to solid state effects.

Acknowledgment. We are indebted to Prof. Peter Pulay and Dr. Jon Baker for helpful discussions and advice concerning the new scaling technique discussed in ref 28. We thank the National Science Foundation (CHE-9601976, DMR-9501325, DMR-9802300, DMR-9803025) for support and the National Center for Supercomputing Applications (NCSA, No. CHE-970017N) for the use of supercomputing facilities.

Supporting Information Available: Two figures of high-resolution infrared transmission spectra of high purity C_{60} single crystals with the new assignments, one table of calculated vibrational frequencies using seven different methods, and the Excel table of the data shown in Figure 3. This material is available free of charge via the Internet at http://pubs.acs.org.

References and Notes

(1) Kroto, H. W.; Heath, J. R.; O'Brien, S. C.; Curl R. F.; Smalley, R. E. *Nature* **1985**, *318*, 162.

(2) (a) Krätschmer, W.; Fostiropoulos, K.; Huffman, D. R. *Chem. Phys. Lett.* **1990**, *170*, 167. (b) Faufler, R. E.; Conceicao, J.; Chibante, L. P. F.; Chai, Y.; Byrne, N. E.; Flanagan, S.; Haley, M. M.; O'Brien, S. C.; Pan, C.; Xiao, Z.; Billups, W. E.; Ciufolini, M. A.; Hauge, R. H.; Margrave, J. L.; Wilson, L. J.; Curl, R. F.; Smalley, R. E. *J. Phys. Chem.* **1990**, *94*, 8634. (c) Bethune, D. S.; Meijer, G.; Tang, W. C.; Rosen, H. J.; Golden, W. G.; Seki, H.; Brown, C. A.; de Vries, M. S. *Chem. Phys. Lett*. **1991**, *179*, 181. (d) Brüesch, P. *Phonons: Theory and Experiments II*; Springer Ser. Solid State Sci.; Springer: Berlin, 1986; Vol. 65, (e) Bethune, D. S.; Meijer, G.; Tang, W. C.; Rosen, H. J.; Golden, W. G.; Seki, H.; Brown, C. A.; Derries, M. S. *Chem. Phys. Lett*. **1991**, *179*, 181. (f) Pichler, T.; Matus, M.; Kurti, J.; Kuzmany, H. *Phys. Rev. B* **1992**, *45*, 13841. (g) Coulombeau, C.; Jobic, H.; Bernier, P.; Fabre, C.; Schütz, D.; Rassat, A. *J. Phys. Chem*. **1992**, *96*, 22.

(3) (a) Lynch, K.; Tanke, C.; Menzel, F.; Brockner, W.; Scharff, P.; Stumpp, E. *J. Phys. Chem*. **1995**, *99*, 7985. (b) Brockner, W.; Menzel, F. *J. Mol. Struct*. **1996**, *378*, 147.

(4) (a) Gallagher, S. H.; Armstrong, R. S.; Lay, P. A.; Reed, C. A. *Chem. Phys. Lett.* **1996**, *248*, 353. (b) Gallagher, S. H.; Armstrong, R. S.; Bolskar, R. D.; Lay, P. A.; Reed, C. A. *J. Mol. Struct*. **1997**, *407*, 81.

(5) (a) Gensterblum, G.; Pireaus, J. J.; Thiry, P. A.; Caudono, R.; Vigneron, J. P.; Lambin, Ph.; Lucas, A. A.; Krätschmer, W. *Phys. Rev. Lett*. **1991**, *67*, 2171. (b) Prassides, K.; Dennis, T. J. S.; Hare, J. P.; Tomkinson, J.; Kroto, H. W.; Taylor, R.; Walton, D. R. M. *Chem. Phys. Lett*. **1991**, *187*, 455. (c) Neumann, D. A.; Copley, J. R. D.; Kanntakahara, W. A.; Rush, J. J.; Cappelletti, R. L.; Coustel, N.; Fisher, J. E.; McCauley, J. P.; Smith, A. B.; Kreegan, K. M.; Cox, D. M. *J. Chem. Phys*. **1992**, *96*, 8631.

(6) Wang, K. A.; Rao, A. M.; Eklund, P. C.; Dresselhaus, M. S.; Dresselhaus, G. *Phys. Rev. B*. **1993**, *48*, 11375.

(7) Martin, M. C.; Du, X.; Kwon, J.; Mihaly, L. *Phys. Rev. B* **1994**, *50*, 173.

(8) Martin, M. C.; Fabian, J.; Gidard, J.; Bernier, P.; Lambert, J. M.; Mihaly, L. *Phys. Rev. B* **1995**, *51*, 2894.

(9) Nissen, M. K.; Wilson, S. M.; Thewalt, M. L. W. *Phys. Rev. Lett*. **1992**, *69*, 2423.

(10) Heid, R.; Pintschovius, L.; Godard, J. M. *Phys. Rev*. **1997**, *B56*, 5925.

(11) (a) Sassara, A.; Zerza, G.; Chergui, M. *J. Phys. B*, **1996**, *29*, 4997. (b) Sassara, A.; Zerza, G.; Chergui, M. *Chem Phys. Lett.*, **1996**, *261*, 213.

(12) Mihaly, L., et al. In *Progress in Fullerene Science*; Kuzmany, H., Fink, J., Mehring, M., Roth, S., Eds.; World Scientific: Singapore, 1995; p 265.

(13) Long, V. C.; Musfeldt, J. L., Kamaras, K.; Schilder, A.; Schutz, W. *Phys. Rev*. **1998**, *B58*, 14338.

(14) Cardini, G.; Bini, R.; Salvi, P. R.; Schettino, V.; Klein, M. L.; Strongin, R. M.; Brard, L.; Smith, A. B. III, *J. Phys. Chem.* **1994**, *98*, 9966.

(15) Haddon, R. C.; Hebard, A. F.; Rosseinsky, M. J.; Murphy, D. W.; Duclos, S. J.; Lyons, K. B.; Miller, B.; Rosamilia, J. M.; Fleming, R. M.; Kortan, A. R.; Glarum, S. H.; Mahija, A. V.; Muller, A. J.; Eick, R. H.; Zahurak, S. M.; Tycko, R.; Dabbagh, G.; Thiel F. A. *Nature* **1991**, *350*, 320.

(16) Hebard, A. F.; Rosseinsky, M. J.; Haddon, R. C.; Murphy, D. W.; Glarum, S. H.; Palstra, T. T. M.; Ramirez, A. P.; Kortan, A. R. *Nature* **1991**, *350*, 600.

(17) (a) Rao, A. M.; Zhou, P.; Wang, K.; Hager, G. T.; Holden, J. M.; Wang, Y.; Lee, W. T.; Bi, X.; Eklund, P. C.; Cornett, D. S.; Duncan, M. A.; Amster, I. J. *Science*, **1993**, *259*, 955. (b) Iwasa, Y.; Arima, T.; Fleming, R. M.; Siegrist, T.; Zhou, O.; Haddon, R. C.; Rothberg, L. J.; Byons, K. B.; Carter, H. L., Jr.; Hebard, A. F.; Tycko, R.; Dabbagh, G.; Krajewski, J. J.; Thomas, G. A.; Yagi, T. *Science* **1994**, *264*, 1570. (c) Pekker, S.; Jánossy, A.; Mihaly, L.; Chauvet, O.; Carrard, M.; Forró, L. *Science* **1994**, *265*, 1077.

(18) Stephens, P. W.; Mihaly, L.; Lee, P. L.; Whetten, R. L.; Huang, S. M.; Kaner, R.; Deiderich, F.; Holczer, K. *Nature* **1991**, *351*, 632.

(19) (a) Duclos, S. J.; Haddon, R. C.; Glarum, S.; Hebard, A. F.; Lyons, K. B. *Science* **1991**, *254*, 1625. (b) Prassides, K.; Tomkinson, J.; Christides, C.; Rosseinsky, M. J.; Murphy, D. W.; Haddon, R. C. *Nature* **1991**, *354*, 462. (c) Eklund, P. C.; Zhou, P.; Wang, K. A.; Dresselhaus, G.; Dresselhaus, M. S. *J. Phys. Chem*. **1992**, *53*, 1391. (d) Zhou, P.; Wang, K. A.; Wang, Y.; Eklund, P. C.; Dresselhaus, G.; Jishi, R. A. *Phys. Rev. B* **1992**, *46*, 2595.

(20) (a) Fu, K.-J.; Karney, W. L.; Chapman, O. L.; Huang, S.-M.; Kaner, R. B.; Diederich, F.; Holczer, K.; Whetten, R. L. *Phys. Rev. B* **1992**, *46*, 1937. (b) Pichler, T.; Winkler, R.; Kuzmany, H. *Phys. Rev. B* **1994**, *49*, 15879. (c) Kuzmany, H.; Winkler, R.; Pichler, T. *J. Phys. Condens. Matter* **1995**, *7*, 6601.

(21) Rice, M. J.; Choi, H. Y. *Phys. Rev. B* **1992**, *45*, 10173.

(22) Weeks, D. E.; Harter, W. G. *Chem. Phys. Lett*. **1988**, *144*, 366.

(23) (a) Stanton, R. E.; Newton, M. D. *J. Phys. Chem*. **1988**, *92*, 2141. (b) K. Raghavachari and C. M. Rohlfing, *J. Phys. Chem*. **1991**, *95*, 5768.

(24) Negri, F.; Orlandi, G.; Zerbetto, F. *J. Am. Chem. Soc*. **1991**, *113*, 6037.

(25) Jishi, R. A.; Mirie, R. M.; Dresselhaus, M. S. *Phys. Rev. B* **1992**, *45*, 13685.

(26) (a) Wang, X. Q.; Wang, C. Z.; Ho, K. M. *Phys. Rev. B* **1993**, *48*, 1884. (b) Giannozzi, P.; Baroni, S. *J. Chem. Phys*. **1994**, *100*, 8537. (c) Quong, A. A.; Pederson, M. R.; Feldman, J. L. *Solid State Commun*. **1993**, *87*, 535.

(27) Sanguinetti, S.;. Benedek, G.; Righetti, M.; Onida, G. *Phys. Rev. B* **1994**, *50*, 6743.

(28) Baker, J.; Jarzecki, A. A.; Pulay, P. *J. Phys. Chem. A* **1998**,*102*, 1412.

(29) (a) Pulay, P.; Török, F.; *J. Mol. Struct*. **1975**, *29*, 1123. (b) Blom, C. E.; Altona, C., *Mol. Phys*. **1977**, *33*, 875. (c) Pulay, P.; Fogarasi, G.; Pongor, G.; Boggs, J. E.; Vargha, A. *J. Am. Chem. Soc*. **1983**, *105*, 7037.

(30) (a) Dixon, D. A.; DeKock, R. L. *J. Chem. Phys*. **1992**, *97*, 1157. (b) Fan, L.; Ziegler, T. *J. Chem. Phys*. **1992**, *96*, 9005. (c) Murray, C. W.; Laming, G. J.; Handy, N. C.; Amos, R. D. *J. Phys. Chem*. **1993**, *97*, 1868. (d) Chong, D. P.; A. V. Bree, *Chem. Phys. Lett*. **1993**, *210*, 443. (e) Stirling, A.; Papai, I.; Mink, J.; Salahub, D. R. *J. Chem. Phys*. **1994**, *100*, 2910. (f) Stephens, P. J.; Devlin, F. J.; Chabalowski, C. F.; Frisch, M. J. *J. Phys. Chem*. **1994**, *98*, 11623. (g) Rauhut, G.; Pulay, P. *J. Phys. Chem.* **1995**, *99*, 3093. (h) Johnson, B. G.; Florian, J. *Chem. Phys. Lett*, **1995**, *247*, 120. (i) Choi, C. H.; Kertesz, M. *J. Phys. Chem*. **1996**, *100*, 16530. (j) Choi, C. H.; Kertesz, M. *J. Phys. Chem. A* **1997**, *101*, 3823.

(31) See e.g. Pulay, P.; Fogarasi, G.; Pang, F.; Boggs, J. E. *J. Am. Chem. Soc.* **1979**, *101*, 2550. Pulay, P. *J. Mol. Struct*. **1995**, *347*, 293.

(32) Panchenko, Y. N.; De Marè, G. R.; Pupyshev, V. I. *J. Phys. Chem*. **1996**, *17*, 49.

(33) (a) Cuff, L.; Cui, C.; Kertesz, M. *J. Am. Chem. Soc*. **1994**, *116*, 9269. (b) Cuff, L.; Kertesz, M. *Macromolecules*, **1994**, *27*, 762. (c) Cuff, L.; Kertesz, M. *J. Chem. Phys*. **1997**, *106*, 839. (d) Choi. C. H.; Kertesz, M. *Macromolecules* **1997**, *30*, 620−630.

(34) Wilson, W. B., Jr.; Decius, J. C.; Cross, P. C. *Molecular Vibrations*; McGraw-Hill: New York, 1955.

(35) Pulay, P.; Fogarasi, G. *J. Chem. Phys.* **1992**, *96*, 2856.

(36) Press, W. H.; Flannery, B. P.; Teukolsky, S. A.; Vetterlang, W. T. *Numerical Recipes*; Cambridge University, Cambridge, UK, 1989.

(37) Hohenberg, P.; Kohn, W. *Phys. Rev. B* **1964**, *136*, 864.

(38) Becke, A. D. *Phys. Rev.* **1988**, *A 38*, 3098.

(39) Becke, A. D. *J. Chem. Phys.* **1993**, *98*, 5648.

(40) Lee, C.; Yang, W.; Parr, R. G. *Phys. Rev B* **1988**, *37*, 785.

(41) *Gaussian 94*, Revision C.2; Frisch, M. J.; Trucks, G. W.; Schlegel, H. B.; Gill, P. M. W.; Johnson, B. G.; Robb, M. A.; Cheeseman, J. R.; Keith, T. A.; Petersson, G. A.; Montgomery, J. A.; Raghavachari, K.; Al-Laham, M. A.; Zakrzewski, V. G.; Ortiz, J. V.; Foresman, J. B.; Cioslowski, J.; Stefanov, B. B.; Nanayakkara, A.; Challacombe, M.; Peng, C. Y.; Ayala, P. Y.; Chen, W.; Wong, M. W.; Andres, J. L.; Replogle, E. S.; Gomperts, R.; Martin, R. L.; Fox, D. J.; Binkley, J. S.; Defrees, D. J.; Baker, J.; Stewart, J. J. P.; Head-Gordon, M.; Gonzalez, C.; Pople, J. A. Gaussian, Inc.: Pittsburgh, PA, 1995.

(42) Person, W. B., Zerbi, G., Eds. *Vibrational Intensities in Infrared and Raman Spectroscopy*; Elsevier: Amsterdam, 1982.
(43) Choi, C. H. *QCPE* **1997**, *17(3)*, QCMP176
(44) (a) Disch, R. L.; Schulman, J. M.*Chem. Phys. Lett*. **1986**, *125*, 465. (b) Negri, F.; Orlandi, G.; Zerbetto, F. *Chem. Phys. Lett*. **1988**, *144*, 31. (c) Scuseria, G. *Chem. Phys. Lett*. **1991**, *176*, 423. (d) Martins, J. L.; Troullier, N.; Weaver, J. H. *Chem. Phys. Lett*. **1991**, *180*, 457. (e) Häser, M.; Almlöf, J.; Scuseria, G. E. *Chem. Phys. Lett*. **1991**, *181*, 497.
(45) (a) Andreoni, W.; Gygi, F.; Parrinello, M. *Phys. Rev. Lett*. **1992**, *68*, 823. (b) Andreoni, W.; Giannozzi, P.; Parrinello, M. *Phys. Rev. B* **1995**, *51*, 2087.
(46) (a) Yannoni, C. S.; Bernier, P. P.; Bethune, D. S.; Meijer, G.; Salem, J. R. *J. Am. Chem. Soc*. **1991**, *113*, 3190. (b) Hawkins, J. M.; Meyer, A.; Lewis, T. A.; Loren, S.; Hollander, F. J. *Science* **1991**, *252*, 312.
(47) Allen, K. M.; David, W. I. F.; Fox, J. M.; Ibberson, R. M.; Rosseinsky, M. J. *Chem. Mater*. **1995**, *7*, 764.
(48) Bohnen, K.-P.; Heid, R.; Ho K.-M.; Chan, C. T. *Phys. Rev*. **1995**, B51, 5805.
(49) Coulombeau, C., et al. *Fullerene Sci. Technol.* **1994**, *2*, 247 as cited in Pintschovius, L. *Rep. Prog. Phys.* **1996**, *59*, 473.
(50) Procacci, P.; Cardini, G.; Salvi, P. R.; Marconi, G. *Mol. Cryst. Liq. Cryst*. **1993**, *229*, 75.